
CHALMERS
UNIVERSITY OF TECHNOLOGY

# Verification of a Transient Model for the Simulation of Curve Squeal on the Basis of On-Board Noise Monitoring Data from Stockholm Metro

# Verification of a Transient Model for the Simulation of Curve Squeal on the Basis of On-Board Noise Monitoring Data from Stockholm Metro

Astrid Pieringer[1], Peter Torstensson[2]

[1] *Division of Applied Acoustics, Chalmers University of Technology, SE-41296 Göteborg, Sweden,*
*Email: astrid.pieringer@chalmers.se*

[2] *Swedish National Road and Transport Research Institute (VTI), SE-40278 Göteborg, Sweden,*
*Email: peter.torstensson@vti.se*

## Introduction

Curve squeal is an intense tonal noise emitted by railway vehicles negotiating tight curves. It is attributed to self-excited vibrations of the railway wheel during 'imperfect' curving [1]. Modelling curve squeal poses a challenge since the phenomenon is non-linear and transient. Also curve squeal measurements are challenging since the phenomenon is rather chaotic than deterministic. Squeal probability varies for nominally identical vehicles and also depends on the environmental conditions that vary from day to day or even hour to hour [1]. Curve squeal also depends on parameters that are difficult to control and measure in field measurements such as the local friction conditions in the wheel/rail contact and the contact positions on wheel and rail. As a consequence, it is also difficult to validate curve squeal models. This work partly addresses both modelling of curve squeal, squeal measurements and validation of curve squeal models. A previously developed model for the simulation of curve squeal during transient curving [2, 3] is verified based on on-board noise monitoring data from Stockholm metro [4]. Simulations with the model are also used to analyse the measurement data.

## Transient curve squeal model

The squeal model used in this work is the time-domain model WERAN (WhEel/RAil Noise) for wheel/ rail interaction and noise [2, 3] that combines pre-calculated impulse response functions (Green's functions) for track and wheel dynamics with an implementation of Kalker's variational method for transient rolling contact [5]. The model includes the coupling between vertical and lateral dynamics of wheel and track and considers squeal in the case of a constant friction coefficient. Longitudinal dynamics is not included. Varying contact conditions along the curve such as varying contact position on wheel and rail, varying friction and varying creepages can be included [3]. The low-frequency curving behaviour is considered by a pre-calculation with the vehicle dynamics software SIMPACK [8]. The time series of the contact positions on wheel and rail and the creepages calculated with SIMPACK serve as input to WERAN for the squeal simulations.

In this study, vehicle and track are modelled on the basis of the conditions at the Stockholm metro. The track superstructure includes continuously welded BV50 rails (50 kg/m) with inclination 1:40 mounted via Pandrol pads to monoblock sleepers on ballast subgrade. The vehicles are C20 trains manufactured by Bombardier Transportation. Trains at the Stockholm metro use S1002 wheel profiles.

In WERAN, the vehicle is represented by a single flexible C20 metro wheel with a radius of 390 mm, which is modelled using a commercial finite element software. A rigid constraint is applied at the inner edge of the hub, where the wheel would be connected to the axle. With this undamped FE model, the eigenfrequencies and eigenmodes have been calculated up to 7 kHz. The eigenmodes of the wheel were assigned a modal damping value using the approximate values proposed by Thompson [6]. From this modal basis, the Green's functions of the wheelset were calculated. The track model consists of one continuously supported rail of type BV50 and is built with waveguide finite elements using an inhouse software [7]. Track receptances calculated for various combinations of excitation and response points on the rail are used to construct the moving Green's functions of the track, which inlcude the motion of the contact point along the rail with train speed [2]. The material data of the wheel and track are given in [2].

## Curve squeal monitoring

In previous work, a statistical analysis was carried out based on longterm onboard noise monitoring data collected on Stockholm metro. The methodology and results are in detail described in [4] and are shortly summarized here. Microphones are mounted close to the wheels of one wheelset on several Bombardier C20 trainsets. Data from two such vehicles that have operated in regular traffic on the Green line in Stockholm between January 2019 and November 2021 are used. A passage through a curve is identified as squealing if the radiated noise from the inner wheel exceeds that of the outer wheel by at least 3 dB(A) during a continuous time interval of at least 0.5 s. In total, 143 curves both inside and outside tunnels and 379 776 vehicle passages have been considered.

A binary logistic regression analysis has been carried out on the data. The following model has been adapted to the data of each curve separately

$$\text{logit}(s) = \ln \frac{s}{1-s} = \theta_0 + \theta_1 x_1 + \theta_2 x_2 + \theta_3 x_3 + \theta_4 x_4 + \theta_5 x_1 x_3 + \theta_6 x_3 x_4 \,, \quad (1)$$

where $\theta_n$ are regression coefficients, $s$ is the probability for curve squeal and the explanatory variables $x_1$ $x_2$ , $x_3$

and $x_4$ are, respectively, vehicle individual, rail grinding, air temperature and air relative humidity. In 122 of the 143 curves, regression coefficients could be estimated. All results of the analysis are presented in [4]. Only two of the results are repeated here.

Figure 1 shows the estimated regression coefficient $\theta_0$, also denoted intercept, for each curve as a function of curve radius. "It shows that curve squeal has a generally higher probability for smaller radius curves but also that this effect levels off at around 600 m radius. Curve radius is not introduced as a separate explanatory variable in the analysis but the tilt in the distribution shown in [Figure 1] demonstrate that shorter radius covary with higher squeal probability. Also, results obtained for curves outdoors and in tunnels are observed in one common cloud which suggest the impact of location to be unimportant." [4].

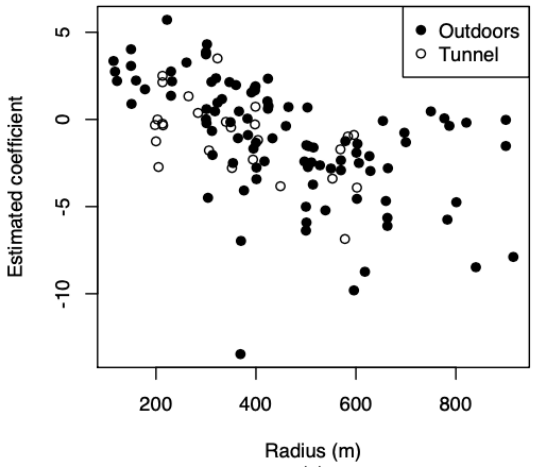


**Figure 1:** Results from the regression analysis of vehicle passages through 122 curves inside and outside tunnels. Intercept $\theta_0$ (denoted 'estimated coefficient') as a function of curve radius. Reprinted from [4].

The other result repeated here concerns the influence of rail grinding on the probability of curve squeal. Rail grinding is necessary from time to time to restore the rail profile and to remove surface defects and irregularities such as severe corrugation, see Figure 2. "For curves that were ground during the studied period a dummy variable is introduced. In the analysis, squeal occurrence for vehicle passages performed before/after grinding is treated separately. The resulting coefficients are found in [Figure 3]. The cloud is centered above 0 which indicates an increased probability for curve squeal after rail grinding." [4].

## Squeal simulations

Simulations with WERAN have been carried out to replicate and analyse the results from the regression analysis of noise monitoring data presented in the previous section. This also serves as a verification of the squeal model.

**Figure 2:** Example of rail corrugation from a curve in the network of Stockholm metro.

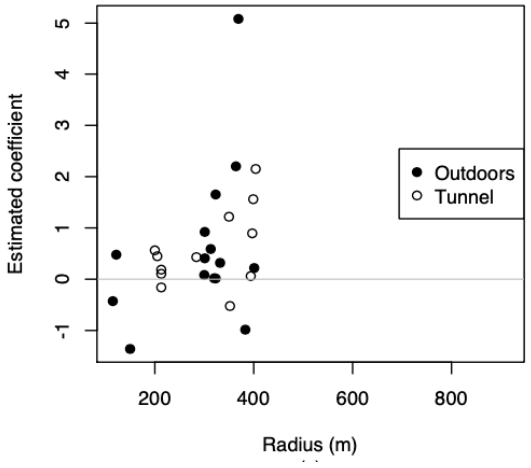


**Figure 3:** Results from the regression analysis of vehicle passages through 27 curves inside and outside tunnels that were ground during the period of investigation. Estimated regression coefficient for rail griding $\theta_2$ (denoted 'estimated coefficient') as a function of curve radius. Reprinted from [4].

### *Influence of the curve radius*

In a first step, a parameter study was carried out to investigate the influence of curve radius on the occurrence of curve squeal. The low-frequency curving behaviour of a C20 vehicle was first calculated with SIMPACK considering a transition curve of 50 m length and a circular curve of 100 m length of BV50 track. The calculated contact positions on wheel and rail and the lateral creepage at the leading inner wheel in the leading bogie of the vehicle in the circular curve then served as input to WERAN for the high-frequency squeal simulation. Rail profile, friction coefficient and train speed were kept constant throughout the curve. The wheel and rail profiles used were a nominal S1002 profile and a nominal BV50 profile, respectively. Five different curve radii, three different friction coefficients and three different velocities were considered in the study resulting in 45 different parameter combinations. The curve radii included 100 m, 300 m, 500 m, 700 m, and 900 m, the friction coefficients 0.20, 0.35 and 0.50 and the velocities 0.75 $v_{\mathrm{eq}}$ , $v_{\mathrm{eq}}$

and 1.25 $v_{\mathrm{eq}}$, where $v_{\mathrm{eq}}$ is the equilibrium speed of the respective curve. The SIMPACK results are presented in Figure 4 in terms of the lateral creepage and in Figure 5 in terms of the wheel/rail contact positions. It is seen that the lateral creepage increases with decreasing curve radius. Especially in the 100 m radius curve, a high creepage occurs. In the 300 m curve, the creepage is still elevated while it is low in longer radius curves. The lateral creepage only depends slightly on friction coefficient and train speed, with a bit higher influence of the friction coefficient in comparison to the train speed. The wheel/rail contact position seen in Figure 5 is almost identical for all parameter combinations. The contact on the rail occurs in the middle of the rail profile, the contact on the wheel more towards the field side. The results of the subsequent squeal simulations with WERAN are depicted in Figure 6 in the form of a single value measure $L_{F_2}$. The measure $L_{F_2}$ is calculated from the rms-value of the transient part of the last 0.15 s of the lateral contact force [2] :

$$L_{F_2} = 20 \log \frac{F_{2,\mathrm{rms}}}{1\,\mathrm{N}} \,. \tag{2}$$

The total simulated signals in WERAN are 3.5 s long.

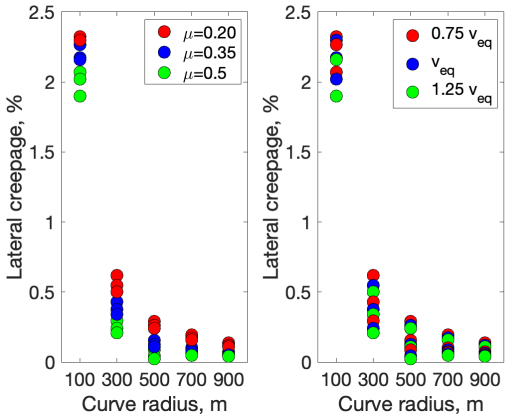


**Figure 4:** Lateral creepage at the leading inner wheel in the leading bogie of a C20 vehicle in a circular BV50 curve calculated with SIMPACK. The results are given as a function of curve radius, friction coefficient (*left figure*) and train speed (*right figure*).

If squeal does not develop the lateral contact force approaches a constant value, giving low values of $L_{F_2}$. In cases with squeal, a stick/slip oscillation builds up in the contact, resulting in an $L_{F_2}$ of up to 50 dB. In Figure 6, the colour black corresponds to strong squeal, red to light squeal that takes a long time to build up, and yellow to no squeal. Strong squeal occurs for all cases in the 100 m-radius curve. In the 300 m-radius curve only the case of friction coefficient 0.2 leads to light squeal. In the longer radius curves, squeal does not occur in the simulations. These results agree very well with the results of the regression analysis in Figure 1, where squeal probability increases for smaller radius curves. The simulations also indicate that the reason for the increased squeal probability in smaller radius curves is the increased lateral creepage.

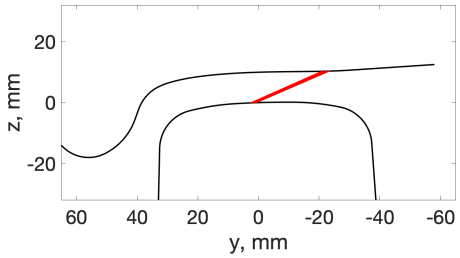


**Figure 5:** Wheel/rail contact positions for all investigated parameter combinations at the leading inner wheel in the leading bogie of a C20 vehicle in a circular BV50 curve calculated with SIMPACK. Almost the same contact positions are obtained for the different parameter combinations.

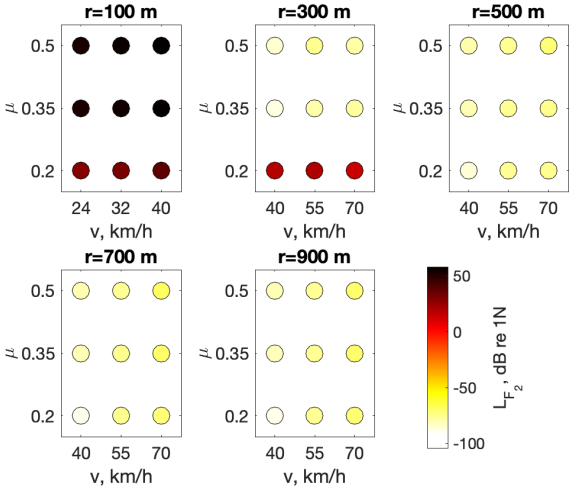


**Figure 6:** Results of the squeal simulations carried out with WERAN for all parameter combinations and nominal wheel/rail profiles. The results are given in terms of the single value measure $L_{F_2}$ calculated from the lateral contact force. Black corresponds to strong squeal, red to light squeal and yellow to no squeal.

## *Influence of rail grinding*

During rail grinding, the rail profile is (in ideal circumstances) restored to the nominal profile and rail corrugation is removed. Both effects could be the reason for an increased squeal probability in the weeks and months after grinding. In the following, only the effect of the changed rail profile is investigated. One pair of worn rail profiles measured just before rail grinding in a 200 m-radius curve at Stockholm metro was available. The parameter study described in the previous subsection was repeated with this pair of rail profiles replacing the nominal rail profiles, i.e. the profiles measured in the 200 m-radius curve were used for all curves. Ideally, the parameter study should have been carried out for many different pairs of worn rail profiles measured in different radius curves, but such data was not available. The SIMPACK results using the available pair of worn rail profiles (not depicted here) were very similar to the results in Figure 4 and 5. As a consequence, also the results of the

squeal simulations were very similar to the results in Figure 6. This means, the used particular worn rail profile did not change the tendency to squeal in the simulations.

It is, however, well known that different wheel/rail profile combinations can lead to changed lateral contact positions on wheel and rail for the same lateral displacement of the wheelset on the track. In the same way, rail corrugation could lead to changed lateral contact positions. To demonstrate the effect of a changed lateral contact position on squeal, squeal simulations have been carried out with a prescribed variation of the contact positions (Figure 7) starting from the case for curve radius 300 m, friction coefficient 0.2 and train speed 55 km/h, where light squeal occurred, see Figure 6. The results of the squeal simulations are given in Figure 8. If the contact position on the wheel is moved from the original contact position at -22 mm further to the field side (i.e. towards negative $y$-values), squeal stops. If the contact position on the wheel is instead moved in the direction of the flange, squeal increases first in strength, before it diminishes again and finally stops from a contact position of 8 mm on the wheel. These results show that squeal occurs for a certain range of contact positions. This could be the reason for an increased squeal probability after rail grinding.

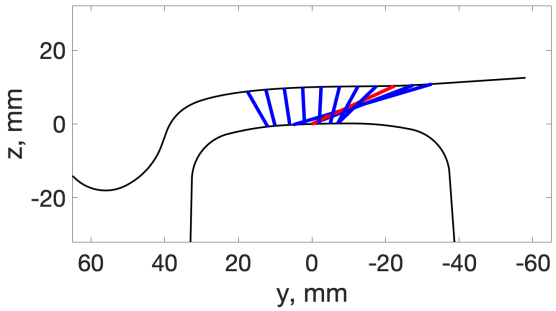


**Figure 7:** Prescribed variation of contact position (*in blue*) in comparison to the original contact position (*in red*).

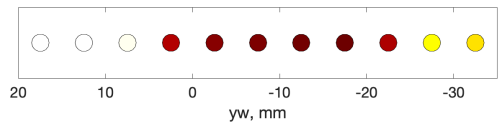


**Figure 8:** Results of the squeal simulations carried out with WERAN for the prescribed variation of contact position shown in Figure 7, curve radius 300 m, friction coefficient 0.2, train speed 55 km/h and nominal wheel/rail profiles. The results are given in terms of the single value measure $L_{F_2}$ calculated from the lateral contact force. The colorbar is found in Figure 6.

## Conclusions

Squeal monitoring data from Stockholm metro has been analysed and partly replicated with a detailed, transient model for curve squeal. The model shows, as the monitoring data, increasing squeal occurrence for decreasing curve radius, which is due to an increasing lateral creepage. Increased squeal occurrence after rail grinding could be due to restored rail profiles or removed corrugation. Simulations showed that a changed lateral contact position (as an effect of changed profiles or corrugation) can lead to an on- and offset of squeal. Further investigations are needed to clarify and explain the influence of rail grinding on curve squeal.

## Acknowledgements

The current study is part of the ongoing activities in CHARMEC - Chalmers Railway Mechanics. It has been funded by the EU's Horizon 2020 research and innovation programme in the project In2Track3 under grant agreement no 101012456 and by the Swedish Transport Administration in the project 'Curve squeal - Influence of track design and maintenance status" (TRV 2020/49829).

## References

[1] Thompson, D.J. , Squicciarini, G., Ding, B., Baeza, L.: A state-of-the-art review of curve squeal noise: Phenomena, mechanisms, modelling and mitigation. In: Noise and Vibration Mitigation for Rail Transportation Systems. NNFM, vol 139, Springer, Cham (2018).

[2] Pieringer, A.: A numerical investigation of curve squeal in the case of constant wheel/rail friction. Journal of Sound and Vibration, 333(18), 4295–4313 (2014).

[3] Pieringer, A, Torstensson, P.T., Theyssen, J., Kropp, W..: Transient modelling of curve squeal considering varying contact conditions, Proceedings of the 14th International Workshop on Railway Noise (IWRN14), Shanghai, China (December 7-9, 2022).

[4] Eriksson, O., Torstensson, P.T., Pieringer, A., Nilsson, R., Höjer, M., Asplund, M., Świerkoska, A.: Survey of curve squeal occurrence for an entire metro system, Proceedings of 14th International Workshop on Railway Noise (IWRN14), Shanghai, China (December 7-9, 2022).

[5] Kalker, J.J.: Three-dimensional elastic bodies in rolling contact. Kluwer Academic Publishers, Dordrecht, Boston, London (1990).

[6] Thompson, D.: Railway noise and vibration: Mechanisms, modelling and means of control, Elsevier, Oxford, UK (2009).

[7] Theyssen, J., Pieringer, A., Kropp, W.: The influence of track parameters on the sound radiation from slab tracks. In Noise and Vibration Mitigation for Rail Transportation Systems edited by Geert Degrande et al., Notes on Numerical Fluid Mechanics and Multidisciplinary Design, 150, 90–97, Springer, Cham (2021).

[8] SIMPACK rail, https://www.3ds.com/products-services/simulia/training/course-descriptions/simpack-rail/ (accessed 29 March 2023).